Theoretical Analysis of UHF Propagation in a City Street Modeled as a Random Multislit Waveguide

Reuven Mazar, Alexander Bronshtein, and I.-Tai Lu, *Senior Member, IEEE*

***Abstract*—In this work, we perform an analysis of a channel for the UHF wave propagation in the city street. The street is modeled as a planar multislit waveguide with screens and slits distributed by a Poisson law. Statistical propagation characteristics in such a waveguide can be expressed in terms of multiple ray fields approaching the observer along a direct ray and the rays reflected by the waveguide walls. The corresponding average field and intensity distributions can be transformed into the sums of mode-like solutions using the Poisson summation formula. Numerical examples are presented and compared with the experimental data.**

***Index Terms*—UHF radio propagation, urban areas.**

I. Introduction

THE design of new highly capable mobile communication systems has created the need to improve and develop new theoretical models for wireless communication channels in dense urban and suburban areas. The identification of typical structures and the design of efficient algorithms for the computation and mapping of the field distribution can provide a useful tool for the optimal design of local communication networks. As a result of the irregular spatial and temporal structure of the urban environments the signal from the transmitter arrives at the receiver along multiple ray trajectories resulting in significant phase and amplitude variations [1]–[4]. In order to perform a detailed analysis of such complex structures, it is appropriate to lay the emphasis on methods that rely on the physical mechanisms of the propagation phenomena while using the experimental data to determine the model's parameters. The statistical analysis is left to the final stage. Recently, such an approach was employed to predict propagation loss in urban environments when the transmitter antenna is located above the buildings [1], [5]. Attempts to reduce the interference level and a consequent increase in the spectral efficiency of the cellular radio communication systems require the reduction of antenna heights. Placing the transmitting and receiving antennas below the rooftops results in a sharp change in the character of propagation where the city street acts as a waveguide channel for the propagating signal. With different approximations, the problem has been studied both theoretically [6]–[12] and experimentally [6], [13], [14]. Propagation along straight streets with irregularly spaced high buildings when the transmitter and the receiver are both located below roof level has been investigated and a statistical waveguide model was applied for computations of the line-of-sight (LOS) attenuation in the city street [15], [16].

In this paper, we extend the waveguide model by employing ray-optical methods [17], [18]. This approach allows us to compute not only the variations of the energetic parameters of the field along the city street, but also to present analytical expressions for the spatial structure of the field.

In Section I, we model the city street as a plane parallel waveguide with a variable reflection coefficient. Using this model we present the field at the observer as a superposition of multiple ray fields traveling from the source. These ray fields can be classified as 1) direct or refracted rays; 2) reflected rays; and 3) rays scattered or diffracted by obstacles such as buildings and the surface of the terrain. In Section II, we consider a waveguide with randomly distributed screens and slits along its boundaries [15], [16] and construct expressions for the average field. The resulting average ray sum can be retransformed into a mode-like solution by using the Poisson sum formula. In Section III, we present algorithms for the average intensity presenting it as a sum of coherent and noncoherent parts. Using the foundations of the geometrical theory of diffraction (GTD) [19]–[23], we show how the diffraction effect of the building corners can be accounted for (Appendix B). Numerical evaluation of the algorithms and comparison with the experimental data is presented in Section IV.

A. Formulation of the Problem

In this section, we apply the ray-optical method for the plane-parallel waveguide with range-dependent reflection coeficients. The propagation geometry is shown in Fig. 1(a) where one boundary of the waveguide is associated with the (yz) plane at $x = 0$ with a reflection coefficient $V_1(z)$ and the parallel plane boundary at $x = h$ with the reflection coefficient $V_2(z)$. The waveguiding system is assumed to be homogeneous in the y-axis direction, with variable reflection coefficients boundaries as functions of z. Since the vertical locations of the transmitter and the receiver are much smaller

Manuscript received January 30, 1997; revised March 16, 1998. This work was supported by The Israel Science Foundation, founded by the Israel Academy of Sciences and Humanities.

R. Mazar and A. Bronshtein are with the Department of Electrical and Computer Engineering, Ben Gurion University of the Negev, Beer Sheva, 84105 Israel.

I.-T. Lu is with the Department of Electrical Engineering and Computer Science, Polytechnic University, Farmingdale, NY 11735 USA.

Publisher Item Identifier S 0018-926X(98)04875-3.

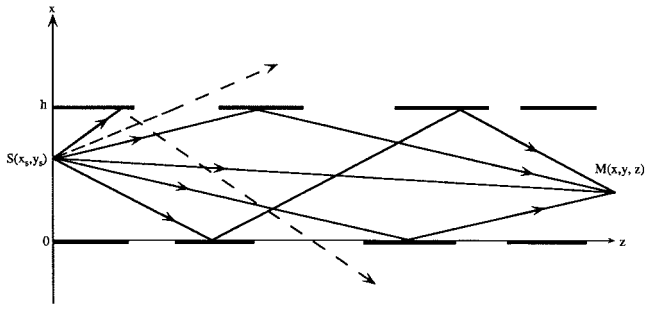

(a)

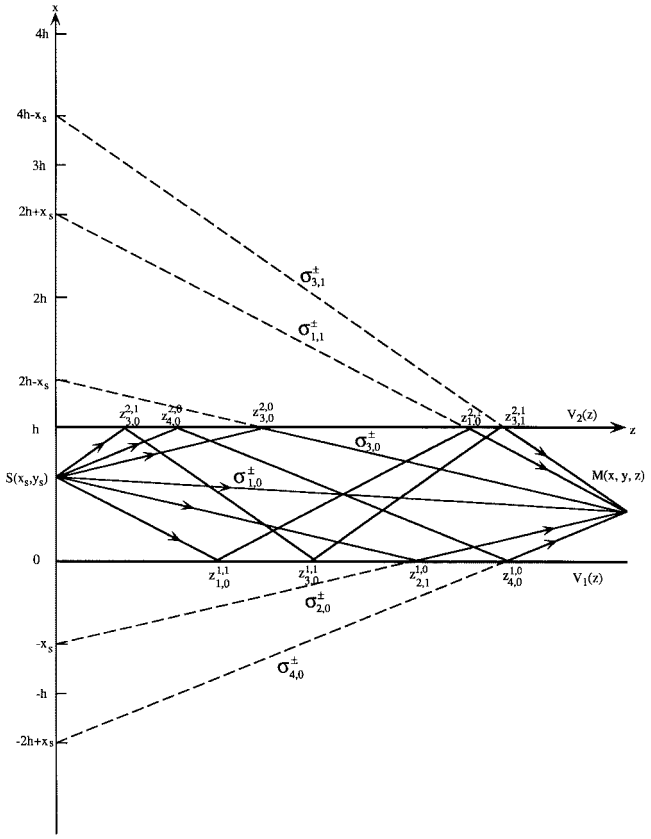

(b)

Fig. 1. (a) Multislit waveguide model of a city street. (b) Image source representation in the plane-parallel waveguide.

compared to the distance z, the y dependence can be neglected. The reflection coefficients are assumed to be also functions of the wavefront incidence angle.

Let us first consider a waveguide which is infinite and homogeneous in the y axis (absence of the ground reflection surface) and with random distribution of slits and screens in the z direction. Then the field $U_f(\mathbf{r}, z)$, $\mathbf{r} = (x, y)$ observed at $M(x, y, z)$ due to a unit strength monochromatic point source at $S(x_s, y_s, 0)$ can be expressed as a sum of several field contributions: 1) field arriving directly from the source at $S(x_s, y_s, 0)$; 2) fields arriving along multiple reflected rays with strengths proportional to the powers of the reflection coefficients of the waveguide boundaries; and 3) single and multiple diffracted fields

$$U_f(x, y, z) = U_r(x, y, z) + U_d(x, y, z) \tag{1}$$

where

$$\begin{aligned} U_r(x,y,z) &= \sum_{m=0}^{\infty} \left\{ \left(\prod_{\mu=0}^{m} V_1(z_{1,\mu}^{1,m}) V_2(z_{1,\mu}^{2,m}) \right) U_{1,m}(x,y,z \mid \sigma_{1,m}^{-}) \right. \\ &\quad + \left(\prod_{\mu=0}^{m} V_1(z_{2,\mu}^{1,m}) V_2(z_{2,\mu}^{2,m}) \right) V_1(z_{2,m+1}^{1,m}) \\ &\quad \times U_{2,m}(x,y,z \mid \sigma_{2,m}^{-}) \\ &\quad + \left(\prod_{\mu=0}^{m} V_1(z_{3,\mu}^{1,m}) V_2(z_{3,\mu}^{2,m}) \right) V_2(z_{3,m+1}^{2,m}) \\ &\quad \times U_{3,m}(x,y,z \mid \sigma_{3,m}^{-}) \\ &\quad \left. + \left(\prod_{\mu=0}^{m+1} V_1(z_{4,\mu}^{1,m}) V_2(z_{4,\mu}^{2,m}) \right) U_{4,m}(x,y,z \mid \sigma_{4,m}^{-}) \right\} \end{aligned} \tag{2}$$

is the contribution of the multiple reflected rays and $U_d(x, y, z)$ is the diffractive term contribution. In general, the amplitudes of the diffracted fields are specified by the incident field amplitude at the corner location and the diffraction coefficients $D_p(\theta_{\mathbf{in}}, \theta_d)$. These diffraction coefficients are determined in the GTD [19], [21]–[23] and are functions of the directional angles $\theta_{\mathbf{in}}$ and θ_d of the incident and diffracted rays. As is shown later in Appendix B, the diffractive contribution can be neglected. In (1), $U_{j,m}(x, y, z \mid \sigma_{j,m}^{\pm})$, $j = 1, \cdots, 4$ are multiple reflected-ray fields arriving from the source $S(x_s, y_s, 0)$ along different rays. The propagation ranges along these rays can be determined from the image source picture [see Fig. 1(b)] and are given by [18]

$$\sigma_{1,m}^{\pm} = \{z^2 + [2mh + x_s - x]^2 + (y_s \pm y)^2\}^{1/2} \tag{3}$$

$$\sigma_{2,m}^{\pm} = \{z^2 + [2mh + x_s + x]^2 + (y_s \pm y)^2\}^{1/2} \tag{4}$$

$$\sigma_{3,m}^{\pm} = \{z^2 + [2(m+1)h - (x_s + x)]^2 + (y_s \pm y)^2\}^{1/2} \tag{5}$$

$$\sigma_{4,m}^{\pm} = \{z^2 + [2(m+1)h - (x_s - x)]^2 + (y_s \pm y)^2\}^{1/2}. \tag{6}$$

There are four indexes in (2) that distinguish the range coordinate $z_{q,\mu}^{p,m}$ for each reflection. Index $p = 1, 2$ denotes either the lower or the upper boundary. Index $q = 1, 2, 3, 4$ is related to the different ray species with ranges (3)–(6), while m for each of these species defines the number of reflections of a given ray. Index μ runs over these reflection events as is seen from Fig. 1(b).

In (1) and (2), we have used the range values $\sigma_{j,m}^{-}$ only. The $\sigma_{j,m}^{+}$ terms will be used later when the ground reflection will be taken into account.

The pathlengths in (3)–(6) are determined by the analogy with a continuous plane-parallel waveguide having ideal reflecting boundaries in which the multiple ray hierarchy can be replaced by an equivalent distribution of real and virtual sources [Fig. 1(b)]. Each virtual source associated with the reflecting rays gives a contribution of $\exp(ik\sigma_{j,m})/(4\pi\sigma_{j,m})$ to the total field at the observer.

B. Average Field Presentation in the Waveguide

In this section, we consider propagation along the street waveguide and construct the average measures assuming that the lengths of the screens L and the slits l are randomly distributed according to the Poisson distribution law: $\frac{1}{L}\exp(-\frac{L}{L})$ and $\frac{1}{l}\exp(-\frac{l}{l})$. Here, $\bar{L}$ and $\bar{l}$ are the average values, respectively. Reflection from the screens is taken into account by introducing the random reflection coefficients $V_1(z)$ and $V_2(z)$ with symbols "1" and "2" denoting the waveguide walls

$$V_i(z)=\begin{cases}\bar{\rho}_i=\rho_i\exp(i\varphi_i), & \text{on the screen,} \quad i=1,2\\ 0, & \text{on the slit.}\end{cases} \tag{7}$$

We note that the reflection coefficient $\bar{\rho}_i$ is generally a complex function which is dependent on the incidence angle and polarization of the wave. The average moments of these functions are [24]

$$\langle V_i(z)\rangle=\chi\bar{\rho}_i=\frac{\bar{L}}{\bar{L}+\bar{l}}\bar{\rho}_i, \quad i=1,2 \tag{8}$$

$$\langle V_i(z_1)V_i(z_2)\rangle=K(z_1,z_2) \tag{9}$$

$$\begin{aligned}&\langle V_i(z_1)V_i(z_2)\cdots V_i(z_n)\rangle\\ &\quad=\langle V_i(z_1)V_i(z_2)\cdots V_i(z_{n-2})\rangle K(z_n,z_{n-1})\end{aligned} \tag{10}$$

where we defined the street structure parameter

$$\chi=\frac{\bar{L}}{\bar{L}+\bar{l}}. \tag{11}$$

The correlation function $K(z_1,z_2)$ is given by [15]

$$\begin{aligned}K(z_1,z_2)=\chi^2\left\{1+\frac{\bar{l}}{\bar{L}}\exp\left[-\left(\frac{1}{\bar{L}}+\frac{1}{\bar{l}}\right)|z_1-z_2|\right]\right\}\\ \times\bar{\rho}_i(z_1)\bar{\rho}_i(z_2).\end{aligned} \tag{12}$$

The distributions of the reflection coefficients of the first and the second street walls are assumed to be statistically independent, i.e.,

$$\langle V_1(z)V_2(z)\rangle=\langle V_1(z)\rangle\langle V_2(z)\rangle. \tag{13}$$

The actual values of the reflection coefficient depend on the ray-incidence angle and the exciting source polarization and is generally a complex number. For sufficiently small glancing angles the reflection coefficient can be approximated as (see Appendix A)

$$\bar{\rho}_i(m)=-\exp(-\gamma_i m) \tag{14}$$

where index m according to (3)–(6) is related to the incidence angle and the coefficient γ_i is a function of source polarization, radiation frequency, and the electrical properties of the reflecting surfaces.

In the case of vertical polarization of the incident electric field with respect to the reflecting surface, the reflection coefficient can be approximated by the general form of (14). In the case of horizontal polarization, the reflection coefficient can be assumed to be real and constant with a value close to -1 [25]. Thus, we can use (14) again, assuming $\gamma=0$.

In addition to the reflected rays there are also fields arriving at the observer along the rays diffracted from the building corners. Because of the random distribution of the slits and screens the terms arising from the diffraction at the street corners add incoherently and their contribution to the average field is negligible.

We apply these assumptions to calculate the average field. Applying an averaging procedure to the expression in (1) and rearranging the terms in (2), we obtain the average field as a sum of two terms in which χ defined in (11) appears as parameter. Denoting the street structure parameter $\chi=e^{-a}$ where a is a any positive number, we obtain the following expression:

$$\left\langle U_f^{td}(x,z)\right\rangle=\frac{1}{4\pi}\{P[x_s-x,0\mid 0]-P[x_s+x,0\mid 1]\} \tag{15}$$

where $P[\Delta x,\Delta y\mid\alpha]$ is defined as

$$\begin{aligned}P[\Delta x,\Delta y\mid\alpha]=\sum_{m=-\infty}^{\infty}\exp\{-|2m+\alpha|a\}\rho(m)^{|2m+\alpha|}\\ \times\frac{\exp\left\{ik\sqrt{z^2+(2mh+\Delta x)^2+\Delta y^2}\right\}}{\sqrt{z^2+(2mh+\Delta x)^2+\Delta y^2}}.\end{aligned} \tag{16}$$

Now we extend the analysis to the three-dimensional case by taking into account the reflection of the ground surface. Here, the average field is a sum of one direct ray and rays that approach the observer after reflection from the waveguide walls plus all the rays that come to the observer after the reflection from the ground surface. The average field can be represented as

$$\begin{aligned}&\langle U_f(x,y,z)\rangle\\ &\quad=\frac{1}{4\pi}\{P[x_s-x,y_s-y\mid 0]-P[x_s+x,y_s-y\mid 1]\\ &\qquad-V_g(P[x_s-x,y_s+y\mid 0]-P[x_s+x,y_s+y\mid 1])\}\end{aligned} \tag{17}$$

where, V_g denotes the ground reflection coefficient which for small glancing angles remains almost constant for both polarizations and can be assumed $V_g=-1$.

In the case of a vertical polarization with respect to the waveguide walls, the ray-field sums in (17) have a rapid convergence because of the fast decay of the reflection coefficient. In the case of the horizontally polarized wave, the convergence of ray-field sums in some cases can be accelerated by applying the Poisson sum formula [17], [18], [26]

$$\sum_{m=-\infty}^{\infty}f(2\pi m)=\frac{1}{2\pi}\sum_{q=-\infty}^{\infty}\int_{-\infty}^{\infty}f(\xi)\exp(iq\xi)\,d\xi. \tag{18}$$

Applying this transformation to each of the sums in (17) and changing the integration variables in the integrals to

$t = \zeta h/\pi + \Delta x$ leads to

$$P[\Delta x, \Delta y \mid \alpha] = \frac{1}{2h}\sum_{q=-\infty}^{\infty}\int_{-\infty}^{\infty}\frac{\exp\left\{ik\sqrt{z^2+\Delta y^2+t^2}\right\}}{\sqrt{z^2+\Delta y^2+t^2}} \times \exp\left(-\frac{|t-\Delta x+\alpha h|a}{h}\right)\exp\left[-\frac{iq(\pi t-\Delta x)}{h}\right]dt. \tag{19}$$

Representing the second exponential term containing the absolute value by its Fourier transform and combining the P terms for $kz \gg 1$ we can approximate (18) as a mode-like expansion with

$$\langle U_f^{\pm}(x,y,z)\rangle = \frac{1}{\pi^2 h}\sqrt{\frac{\pi}{2k}}\frac{\exp\{ik[z^2+y_s\pm y)^2]^{1/2}+i\pi/4\}}{[z^2+(y_s\pm y)^2]^{1/4}} \times \sum_{m=0}^{\infty}\int_{-\infty}^{\infty}\frac{d\xi}{\xi^2+1} \times \exp\left\{-\frac{i[z^2+(y_s\pm y)^2]^{1/2}(\xi a+m\pi)^2}{2kh^2}\right\} \times \sin\left[\frac{m\pi x_s}{h}-\xi a\left(\frac{x_s}{h}-\frac{1}{2}\right)\right] \times \sin\left[\frac{m\pi x}{h}-\xi a\left(\frac{x}{h}-\frac{1}{2}\right)\right]. \tag{20}$$

When the source and the receiver locations satisfy the condition $z \gg |y_s+y|$, the expressions in (16) and (20) can be substantially simplified. Expanding (17) into the Taylor series of $y \pm y_s$, the expression for the average field becomes

$$\langle U_f(x,y,z)\rangle = -2i\sin\left(\frac{ky_s y}{z}\right)\exp\left[\frac{ik(y_s^2+y^2)}{2z}\right]\langle U_f^{td}(x,z)\rangle \tag{21}$$

where $\langle U_f^{td}(x,z)\rangle$ is the average field distribution in the two-dimensional case, i.e., in the absence of the ground surface and in the modal form is represented as

$$\langle U_f^{td}(x,z)\rangle = \frac{1}{\pi^2 h}\sqrt{\frac{\pi}{2k}}\frac{\exp\{ikz+i\pi/4\}}{\sqrt{z}} \times \sum_{m=0}^{\infty}\int_{-\infty}^{\infty}\frac{d\xi}{\xi^2+1}\exp\left\{-\frac{iz(\xi a+m\pi)^2}{2kh^2}\right\} \times \sin\left[\frac{m\pi x_s}{h}-\xi a\left(\frac{x_s}{h}-\frac{1}{2}\right)\right] \times \sin\left[\frac{m\pi x}{h}-\xi a\left(\frac{x}{h}-\frac{1}{2}\right)\right]. \tag{22}$$

In the case of a continuous waveguide ($a = 0$) the expressions in (20) and (22) reduce to the modal expansion of the field [17], [18], [26].

C. Average Intensity

In Appendix B it is shown that the corner diffraction contributions are negligible for most of the practically important propagation ranges. It allows us to approximate the intensity as a square of the absolute value of the field

$$I_f(x,y,z) = |U_f(x,y,z)|^2. \tag{23}$$

Explicitly expanding (23), taking into account the statistical properties of the reflection coefficients, and calculating their statistical moments analogously (as was done for the average field) we can represent the expression for the average intensity as a sum of coherent and noncoherent portions

$$\langle I_f(x,y,z)\rangle = \langle I_c(x,y,z)\rangle + \langle I_{\rm nc}(x,y,z)\rangle. \tag{24}$$

For not very small values of "a" (which is justified for almost all city areas), the contribution to the sums in (17) and (21) comes from the terms with low "m" numbers. Therefore, for $z \gg 2m_{\max}h$, Δx, Δy, the coherent part can be approximated as

$$\langle I_c(x,y,z)\rangle = |\langle U_f(x,y,z)\rangle|^2. \tag{25}$$

The noncoherent portion can be represented by the following formula:

$$\langle I_{\rm nc}(x,y,z)\rangle = \langle I_{\rm nc}^r(x,y,z)\rangle + \langle I_{\rm nc}^d(x,y,z)\rangle \tag{26}$$

where

$$\langle I_{\rm nc}^r(x,y,z)\rangle = \sum_{m=0}^{\infty}\{Q_1 W[2m] + Q_2 W[2(m+1)] + Q_3 W[2m+1] + Q_4 W[2m+1]\} \tag{27}$$

$$Q_j = \frac{1}{(\sigma_{j,m}^-)^2}+\frac{1}{(\sigma_{j,m}^+)^2}-\frac{2\cos[k(\sigma_{j,m}^- - \sigma_{j,m}^+)]}{\sigma_{j,m}^-\sigma_{j,m}^+} \quad j=1,\cdots,4, \tag{28}$$

$$W(m) = [\exp(-a|m|)-\exp(-a|2m|)][\rho(m)]^{2m}. \tag{29}$$

is the noncoherent part due to the reflective terms and $\langle I_{\rm nc}^d(x,y,z)\rangle$ is the noncoherent portion arising due to diffraction from the slit edges. It can be computed by adding the contributions of all edges with corresponding GTD coefficients. An alternative way is presented in Appendix B. According to the results in the case of the vertical polarization this contribution can be neglected for all practically important ranges. In the case of the horizontal polarization, the diffractive sum can be neglected up to the ranges of 1 km. Beyond this range it can be estimated, as shown in Appendix B.

Using the approximation as in (21) for the noncoherent portion and substituting the explicit form of the reflection coeficient, we obtain

$$\langle I_{\rm nc}^r(x,y,z)\rangle = 4\sin^2\left(\frac{ky_s y}{z}\right)\left\{\sum_{m=-\infty}^{\infty}\frac{W(2m)}{z^2+[2mh+(x_s-x)]^2} + \frac{W(2m+1)}{z^2+[2mh+(x_s+x)]^2}\right\}. \tag{30}$$

The coefficient $W(m)$ was defined in (29).

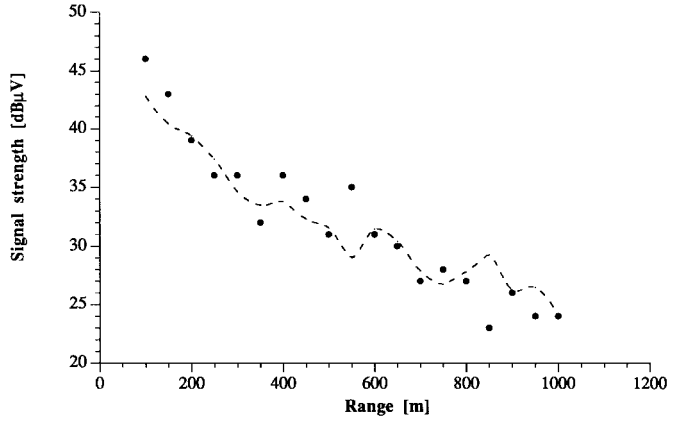

Fig. 2. Signal-strength variation with range z (antenna height 5 m) 870 MHz. Dashed line: theoretical calculations. Points: measurements of [14].

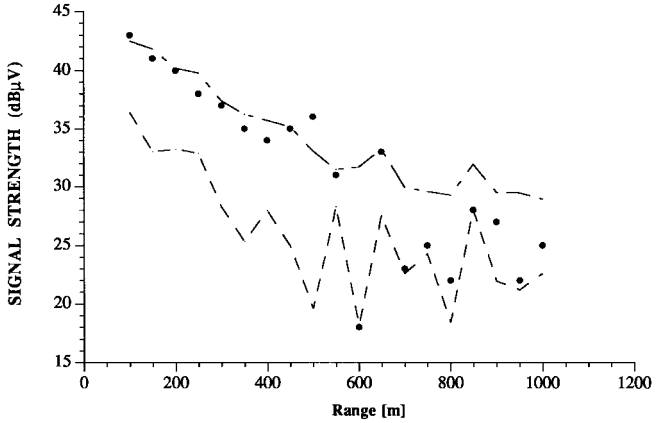

Fig. 3. Field-strength envelope variations with range z (antenna height 9 m) 870 MHz. Dashed line: theoretical calculations. Points: measurements of [14].

D. Numerical Example

To compare the algorithms presented above with experimental data, here we consider a nonregular street waveguide with a street width of $h = 30$ m and choose the street structure parameter $\chi = 0.8$, which was detemined from the data described in [14] and is close to the value characteristic to inner London where the measurements had been performed [13]. The transmitter–receiver configurations were also chosen according to these references.

In Figs. 2–4, we present the signal strength as a function of the range according to direct calculations from (24)–(30). In Fig. 2, the signal dependence is given for the radiation frequency 870 MHz and the transmitting and receiving antenna heights 5 and 1.5 m, respectively. In Fig. 3, the transmitter and the receiver antenna heights were 9 and 1.5 m, respectively. We present the maximum and minimum field-strength amplitude envelopes as functions of range. Since there is a multiple ray contribution, these envelopes were calculated using the assumption of Rayleigh distribution. The results were compared with the measurements performed in [14], while in Fig. 2 we obtain good agreement with the experimenthal data; there is a sharp spread in the measurements presented in Fig. 3 after the range of about 700 m. In Fig. 4, signal path losses were computed for the radiation frequency of 936 MHz, and for the transmitting and receiving antenna heights of 3 and 2 m, respectively. According to recommendations suggested in [25] an averaging interval of 100 wavelengths was used. A comparison with the results of [13] gives good agreement for all propagation ranges. Our results also give the same attenuation rate as in [6].

We note that the algorithms presented in this work can be applied also to the transverse field-distribution computations. For illustration purposes in Fig. 5(a)–(c), we present distributions of the coherent intensity part normalized to the intensity of a direct ray, with a street structure parameter $\chi = 0.5$ for ranges $z = 1$ km, 2 km, 3 km for different source locations. Analyzing the behavior of the coherent part, we note that there is a smoothing of the field pattern with propagation distance, i.e., the contribution of higher modes into the field pattern becomes weaker. This behavior can be easily explained since the higher modes are created by the rays incident on the street boundaries

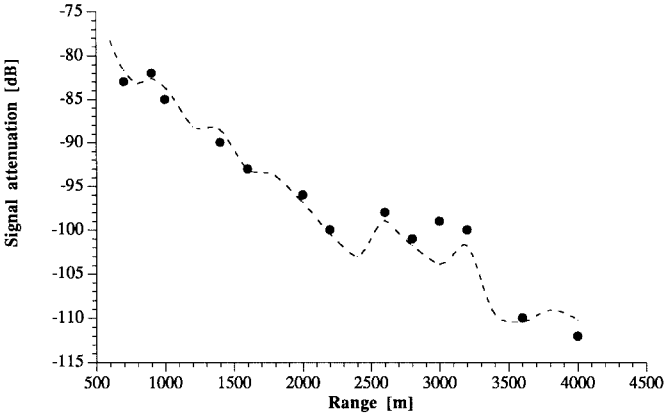

Fig. 4. Path-loss variation with range z 936 MHz. Dashed line: theoretical calculations. Points: measurements of [13].

with higher angles. Since these rays undergo a greater number of reflections, they have a greater escape probability.

Calculating the noncoherent sum, we find that it is almost flat within the waveguide cross section. In Fig. 6, we draw the normalized noncoherent intensity part as a function of the range coordinate z.

II. Summary

In this work, we modeled a city street as a nonregular plane-parallel waveguide and presented the field in it as a superposition of ray fields arriving along straight and multiple reflected random rays. The assumption that the screens and slits on the waveguide walls are distributed according to a Poisson law allowed us to obtain expressions for the average field and the average intensity. Analogously to the continuous plane-parallel waveguide, these expressions can be reduced to mode-like expansions by applying the Poisson sum formula. Analyzing the field structure, we found that higher modes are present in the expression for the average intensity only at short propagation distances. With increasing propagation range, the number of multiple reflected rays dominating the higher order modes decreases, contributing less to the total field and thereby resulting in smoothing.

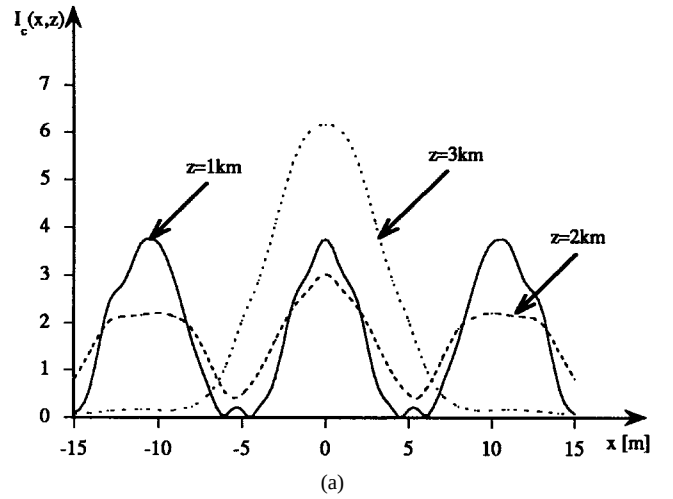

(a)

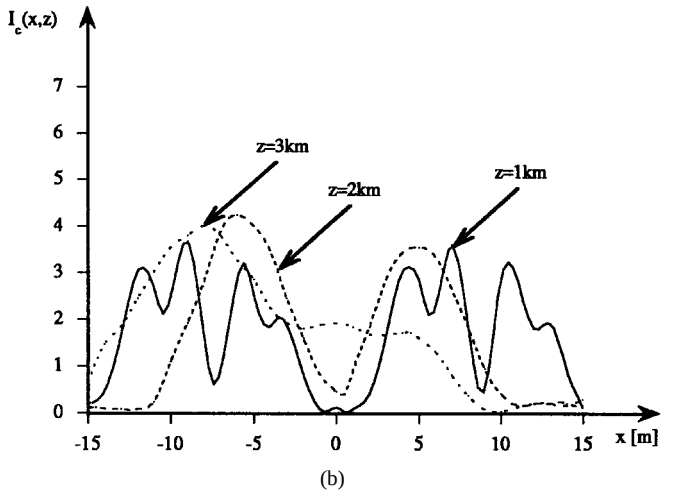

(b)

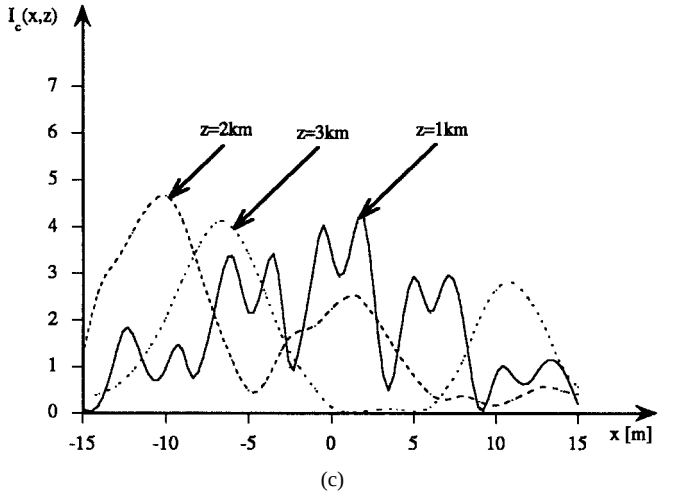

(c)

Fig. 5. Transverse variation of the coherent intensity normalized to the intensity of a direct ray ($\chi = 0.5$) as a function of x for different range planes and source locations. (a) $x_s = 0$. (b) $x_s = 5$ m. (c) $x_s = 10$ m. The middle of the street is at $x = 0$.

We hope that the proposed physical model of the city street will be useful for describing urban propagation channels. The ray approach can be employed to include additional factors affecting the radiowave propagation such as wall roughness and random changes of the refractive index, which are responsible for scattering and fading effects.

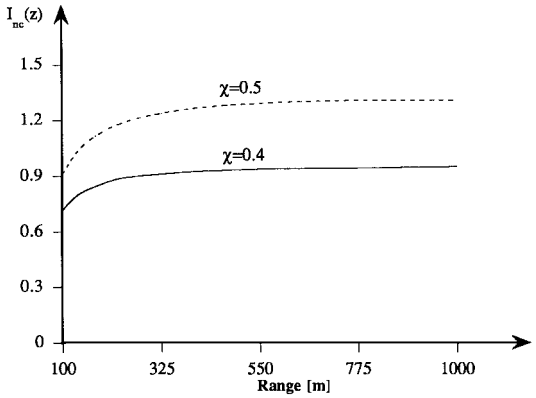

Fig. 6. Variation of the noncoherent intensity normalized to the intensity of a direct ray with range.

APPENDIX A
CALCULATIONS OF THE REFLECTION COEFFICIENT

As indicated in the text, the field from the source arrives at the observer along multiple rays reflected from the walls of the street buildings. The reflection coefficient is dependent on the incidence angle and the E-polarization can be calculated from the well-known formula [25]

$$\rho(m) = \frac{\varepsilon \sin\theta_m - \sqrt{\varepsilon - \cos^2\theta_m}}{\varepsilon \sin\theta_m + \sqrt{\varepsilon - \cos^2\theta_m}} \tag{A.1}$$

where

$$\varepsilon = \varepsilon_r - i\bar{\sigma}; \quad \bar{\sigma} = 60\lambda\sigma$$

$$\sin\theta_m = \frac{mh}{\sqrt{z^2 + (mh)^2}}; \quad \cos\theta_m = \frac{z}{\sqrt{z^2 + (mh)^2}}. \tag{A.2}$$

The real part ε_r of the complex permeability ε represents the dielectric properties of the reflecting material, while σ is related to its conductivity. According to [25] for the urban regions, the typical values are $\varepsilon_r = 3$, $\sigma = 10^{-4}$ \Mhos/m. Then using (A.2), the imaginary part in (A.1) is practically zero and the modulus of $\rho(m)$ can be approximated as

$$|\rho(t)| = \frac{\alpha t^2 - 2t\varepsilon_r\sqrt{\beta} + \beta}{\alpha t^2 + 2t\varepsilon_r\sqrt{\beta} + \beta} \tag{A.3}$$

where we introduced the following notations: $\alpha = \varepsilon_r^2 + \varepsilon_r + \bar{\sigma}^2$, $\beta = \varepsilon_r - 1$, $t = (mh)/z$.

In the case of an irregular waveguide with slits, the number of rays contributing to the field at the observer is limited and decreases with the increase of the street structure parameter χ. For example, when $\chi = 0.8$ (long buildings), the number of important reflections is less then 20. In this case, the phase of the reflection coefficient in (A.3) is nearly constant and its magnitude can be approximated as

$$|\rho(m)| = \exp\{-\gamma m\}, \quad \gamma = \frac{2\varepsilon_r h}{z\sqrt{\varepsilon_r - 1}}. \tag{A.4}$$

In Fig. 7, the approximated reflection coefficient is compared with the exact expression. Good agreement is obtained for all important values of m. We note that (A.4) is applicable also for wider ranges of electrical parameters.

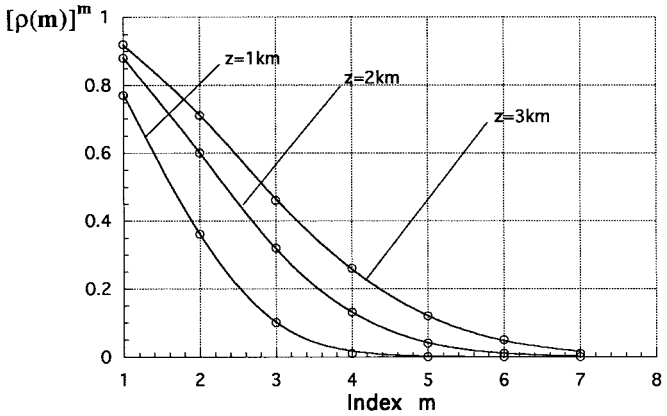

Fig. 7. Approximated reflection coefficient. Solid line: exact calculations. Dots: approximation.

APPENDIX B
CALCULATIONS OF THE CORNER DIFFRACTION CONTRIBUTIONS

The contributions resulting due to diffraction from the street corners can be computed by using the methods of the GTD with given corner diffraction coefficients. This requires taking into account all the diffracted field species and multiple interactions of different reflected and diffracted fields.

For a rough estimate of the magnitude of the diffracted-field contributions, here we adopt the modal approach [22], [27]. Let us first consider a single slit of width $\bar{l}$ in a plane-parallel waveguide without a ground surface. If the slit density is not very high, we can neglect the multiple interaction of the diffracted fields. Let us consider the field in the waveguide as a composition of the intrinsic modes. Since we are dealing with high-frequency radiation $kh \gg 1$ and $k\bar{l} \gg 1$ (where k is the radiation wavenumber and h is the waveguide width) and the fact that the higher order modes have a higher escape probability, we can assume that most of the energy is concentrated in the lower order modes. Each mode propagating in the waveguide interacts with the slit and part of the energy diffracted by the slit edges emerges through the slit and part of it is returned to the waveguide in the form of parasitic modes. Estimates of the amount of energy transfered to the lower order modes show that in the case of the Dirichlet boundary conditions (E-polarization) the relative losses can be approximated as $\delta_{d1} \approx \frac{2}{3}(\frac{\pi\bar{l}}{kh^2})^{3/2}$ and, for the Neuman boundary conditions (H polarization), they can be approximated as $\delta_{d2} \approx \frac{\sqrt{\bar{l}}}{\sqrt{\pi kh}}$.

The distribution function of the parasitic mode amplitudes is given as:

$$\Psi(\eta) = \frac{C}{\eta}\left[\frac{1}{\eta}\int_0^{\eta} \exp(i\xi^2)\, d\xi - 1\right] \tag{B.1}$$

$$\eta = \sqrt{2}k\bar{l}\sin\frac{\phi}{2} = k\bar{l}\sqrt{1-\cos\phi} \tag{B.2}$$

where C is the normalization constant and ϕ is the Brillouin angle of the corresponding mode.

Since the parasitic modes created as a result of diffraction by the street corners add incoherently, their contribution to the incoherent part can be estimated from the energetic considerations. We assume that all propagating coherent modes have the same effectiveness in creating the parasitic modes in the waveguide. This assumption will lead to a higher estimate of the diffracted mode power. The power-balance equations characterizing the dynamics of the coherent field-diffracted field interaction are given by

$$\frac{dP}{dz} = -(\alpha_1 + \alpha_{di})P \tag{B-3}$$

$$\frac{dP_d}{dz} = -\alpha_2 P_d + \alpha_{di}P \tag{B-4}$$

where P is the coherent power propagating along the waveguide, P_d is the power component due to diffraction, α_1 and α_2 are radiation leakage coefficients of the total power and the diffractive part, respectively, and α_{di} is the parasitic mode excitement coefficient defined through the intensity losses per unit length and can be expressed through the coefficients δ_{di} as

$$\alpha_{di} = \frac{2\delta_{di}}{\bar{L}+\bar{l}}. \tag{B.5}$$

Of course, in general, these equations are much more complicated. However, the calculations show, because of the higher mode leakage, the main contribution comes only from the main order modes. Solving the system (B.3), (B.4) and assuming that $\alpha_1 = \alpha_2 = \alpha$ leads to the following result:

$$P(z) = P_0 \exp[-(\alpha + \alpha_{di})z] \tag{B.6}$$

$$P_d(z) = P_0\{\exp(-\alpha z) - \exp[-(\alpha+\alpha_{di})z]\}. \tag{B.7}$$

The relative contribution of the diffractive component can be estimated by analyzing the ratio

$$\frac{P_d(z)}{P(z)+P_d(z)} = 1 - \exp(-\alpha_{di}z). \tag{B.8}$$

We note that with increasing z, (B.8) approaches unity and the whole energy is transmitted to the noncoherent diffractive component. The rate of increase of the diffractive term depends on the parameters α_1, α_2, α_{di}, $\bar{L}$, and $\bar{l}$. For the numerical example, we chose the following values of the parameters: $k = 20$ m^{-1}, $h = 30$ m, $\bar{l} = 20$ m, $\bar{L} = 70$ m. Then, for E polarization we found that the street corner diffractive term can be neglected up to the range of 200 km. For horizontal polarization the diffractive contribution increases more rapidly and has to be taken into account after the range reaches approximately 1 km. Since its contribution is into the noncoherent portion, it can be estimated by using (B.8).

REFERENCES

[1] J. Walfisch and H. L. Bertoni, "A theoretical model of UHF propagation in urban environments," *IEEE Trans. Antennas Propagat.*, vol. 36, pp. 1788–1796, Dec. 1989.
[2] H. L. Bertony, W. Honcharenko, L. R. Maciel, and H. H. Xia, "UHF propagation prediction for wireless personal communications," *Proc. IEEE*, vol. 82, pp. 1333–1359, Sept. 1994.
[3] E. Green, "Radio link design for microcellular systems," *Brit. Telecommun. Technol. J.*, vol. 8, pp. 85–86, 1990.
[4] U. Dersh and E. Zollinger, "Propagation mechanisms in microcell and indoor environments," *IEEE Trans. Veh. Technol.*, vol. 43, pp. 1058–1066, Nov. 1994.
[5] L. R. Maciel, H. L. Bertoni, and H. H. Xia, "Unified approach to prediction of propagation over buildings for all ranges of base station antenna height," *IEEE Trans. Veh. Technol.*, vol. 42, pp. 41–45, Feb. 1993.

[6] A. J. Rustako, N. Amitay, G. J. Owens, and R. S. Roman, "Radio propagation at microwave frequencies for line-of-sight microcellular mobile and personal communications," *IEEE Trans. Veh. Technol.*, vol. 40, pp. 203–210, Feb. 1991.
[7] F. Ikegami, T. Takeuchi, and S. Yoshida, "Theoretical prediction of mean field strength for urban mobile radio," *IEEE Trans. Antennas Propagat.*, vol. 39, pp. 299–302, Mar. 1991.
[8] G. Lampard and T. Vu-Dihn, "The effect of terrain on radion propagation in urban microcells," *IEEE Trans. Veh. Technol.*, vol. 42, pp. 314–317, Aug. 1993.
[9] S. Y. Tan and H. S. Tan, "UTD propagation model in an urban street scene for microcellular communications," *IEEE Trans. Electromagn. Compat.*, vol. 35, pp. 423–428, Nov. 1993.
[10] A. J. Goldsmith and L. J. Greenstein, "A measurement-based model for predicting coverage areas of urban microcells," *IEEE J. Select. Areas Commun.*, vol. 11, pp. 1013–1023, July 1993.
[11] M. C. Lawton and J. P. McGeehan, "The application of deterministic ray launching algorithm for the prediction of radio channel characteristics in small-cell environments," *IEEE Trans. Veh. Technol.*, vol. 43, pp. 955–969, Nov. 1994.
[12] H. H. Xia, H. L. Bertoni, L. R. Maciel, A. Lindsay-Stewart, and R. Row, "Radio propagation characteristics for line-of-sight microcellular and personal communications," *IEEE Trans. Antennas Propagat.*, vol. 40, pp. 1439–1447, Oct. 1993.
[13] K. A. Hughes, "Mobile propagation in London at 936 MHz," *Electron. Lett.*, vol. 18, pp. 141–143, 1982.
[14] P. Harley, "Short distances attenuation measurements at 900 MHZ and 1.8 GHz using low antenna heights for microcells," *IEEE J. Select. Areas Commun.*, vol. 7, pp. 5–11, Jan. 1989.
[15] N. Blaunstein and M. Levin, "VHF/UHF wave attenuation in a city with regularly spaced buildings," *Radio Sci.*, vol. 31, no. 2, pp. 313–323, 1996.
[16] R. Mazar and A. Bronshtein, "Propagation model of a city street for personal and microcellular communications," *Electron. Lett.*, vol. 33, no. 1, pp. 91–93, 1997.
[17] L. B. Felsen and A. H. Kamel, "Hybrid ray-mode formulation of parallel plane waveguide Green's functions," *IEEE Trans. Antennas Propagat.*, vol. AP-29, pp. 637–649, Apr. 1981.
[18] R. Mazar and B. Katz, "Ray-mode analysis of a random medium waveguide," *J. Acoust. Soc. Amer.*, vol. 95, no. 4, pp. 2495–2504, 1994.
[19] J. B. Keller, "Geometric theory of diffraction," *J. Opt. Soc. Amer.*, vol. 52, pp. 116–130, 1957.
[20] L. B. Felsen and N. Marcuwitz, *Radiation and Scattering of Waves*. Englewood Cliffs, NJ: Prentice Hall, 1973.
[21] R. G. Kouyooumjian and P. H. Pathak, "A uniform theory of diffraction for and edge in a perfectly conducting surface," *Proc. IEEE*, vol. 62, pp. 1448–1461, Nov. 1974.
[22] C. A. Borovikov and B. E. Kinber, *Geometrical Theory of Diffraction*. London, U.K.: Inst. Elect. Eng., 1978, vol. 37 (Electromagn. Waves Ser.).
[23] R. C. Hansen, Ed., *Geometric Theory of Diffraction*. New York: IEEE, 1981.
[24] V. I. Klyatskin, *Stochastic Equations and Waves in Randomly Inhomogeneous Media*. Moscow, Russia: Nauka, 1980 (in Russian).
[25] W. C. Y. Lee, *Mobile Communications Engineering*. New York: McGraw-Hill, 1982.
[26] D. S. Ahluwalia and J. B. Keller, "Wave propagation and underwater acoustics," in *Lecture Notes in Physics*, J. B. Keller and J. S. Papadakis, Eds. Berlin, Germany: Springer-Verlag, 1977, vol. 20.
[27] B. Z. Katzenelenbaum, "Diffraction on a plane mirror at the break point in a wide waveguide," *Radiotech. Electron.*, vol. 7, pp. 1111–1119, 1963 (in Russian).

Reuven Mazar was born in Lithuania on January 15, 1949. He received the B.Sc. degree in physics from Technion, Israel Institute of Technology, Haifa, in 1973, the M.Sc. degree in applied physics from Hebrew University, Jerusalem, in 1976, and the Ph.D. degree in engineering from Tel Aviv University, Tel Aviv, Israel, in 1985.

From 1985 to 1987, he was a Research Fellow at the Polytechnic University, Brooklyn, NY. During this stay, he contributed to the formulation of the stochastic geometrical theory of diffraction (SGTD). Presently, he is an Associate Professor in the Department of Electrical and Computer Engineering, Ben-Gurion University of the Negev, Beer-Sheva, Israel. His current research is in wave propagation in complex random environments, imaging in random media, and characterization of wireless communication channels.

Alexander Bronshtein received the B.Sc. and M.Sc. degrees in electrical engineering from Ben-Gurion University of the Negev, Beer-Sheva, Israel, in 1983 and 1991, respectively. He is currently working toward the Ph.D. degree at Ben-Gurion University of the Negev, Beer-Sheva, Israel.

Presently, he is a Radar System Engineer at ELTA Electronics Industries, Ashdod, Israel. His research interests are related to wave propagation in complex random environments with applications to cellular communications, radar systems, and underwater acoustics.

I.-Tai Lu (M'87–SM'95) received the B.S.E.E. degree from National Chiao-Tung University, Hsinchu City, Taiwan, in 1976, the M.S.E.E. degree from National Taiwan University, Taipei, Taiwan, in 1978, and the Ph.D.E.E. degree from Polytechnic University, Brooklyn, NY, in 1985.

From 1978 to 1980, he was an Instructor in the Department of Communication Engineering, National Chiao-Tung University. Presently, he is an Associate Professor of electrical engineering at Polytechnic University. He has published over 45 journal papers, 30 proceeding papers and/or book chapters, given over 20 invited lectures, and conducted over 100 conference/workshop/seminar presentations. His teaching areas are wireless communications, communication networks, wave propagation and scattering, electromagnetic theory, and electronics. His current research interests include wireless communications, underwater and structural acoustics, electromagnetic waves, inverse problems, and signal processing.

Dr. Lu received the N.S.F. Engineering Initiation Awards, Torchlight's Excellent Youth Award, Ministry of Education Award, Award by The Electrical Engineering Foundation of National Taiwan University, as well as awards from the Dai-ichi Kangyo Bank, Ltd., Hong's Foundation for Education and Culture, the Academic Excellency Award by The Alumni Association of National Chiao Tung University, and the County Magistrate's Award. He is a member of Sigma Xi, Commission B of URSI, and the Institute for Theory and Computation of the Electromagnetic Academy. He is listed in *Who's Who Among Asian Americans*, *Who's Who in Science and Engineering*, and is a member of the Acoustical Society of America.